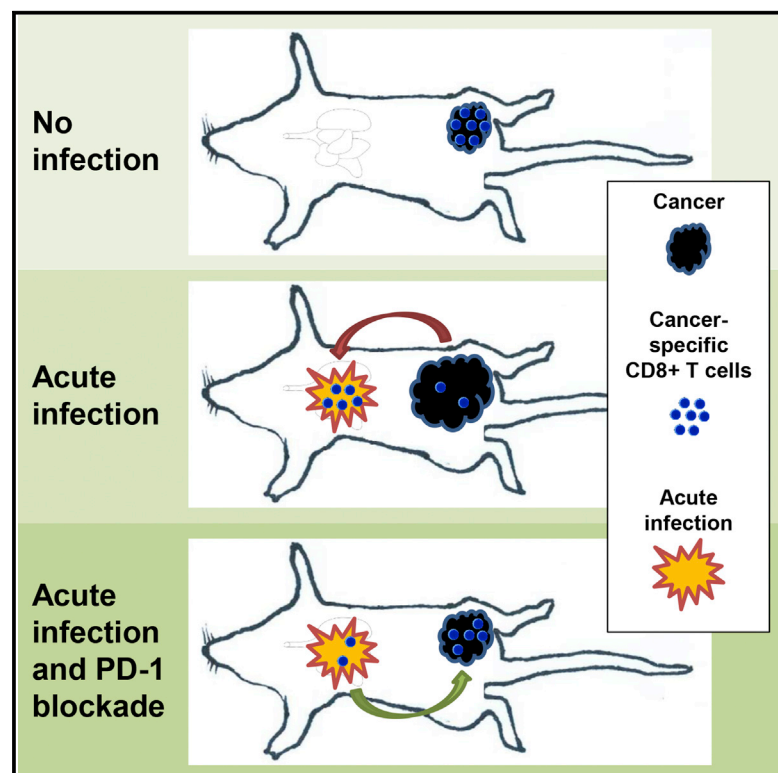# Non-oncogenic Acute Viral Infections Disrupt Anti-cancer Responses and Lead to Accelerated Cancer-Specific Host Death

Graphical Abstract

Authors

Frederick J. Kohlhapp,
Erica J. Huelsmann, Andrew T. Lacek, ...,
Edmund C. Lattime, Howard L. Kaufman,
Andrew Zloza

Correspondence

andrew.zloza@rutgers.edu

In Brief

Kohlhapp et al. report that non-oncogenic infections shunt anti-cancer CD8$^+$ T cells from the tumor to the site of infection and accelerate cancer growth and host death. PD-1 blockade immunotherapy reverses this effect. These findings may explain increased cancer-specific death in patients with cancer-unrelated acute and chronic infections.

Highlights

- Non-oncogenic infections promote distal tumor growth and cancer-specific death

- Infection shunts anti-tumor CD8$^+$ T cells to the site of infection

- Anti-tumor CD8$^+$ T cells express high levels of PD-1 at the infection site

- PD-1 blockade reverses anti-tumor CD8$^+$ T cell loss from the tumor and tumor growth

Report

OPEN
ACCESS
CellPress

Non-oncogenic Acute Viral Infections
Disrupt Anti-cancer Responses
and Lead to Accelerated Cancer-Specific Host Death

Frederick J. Kohlhapp,[1,2,11] Erica J. Huelsmann,[3,11] Andrew T. Lacek,[3,11] Jason M. Schenkel,[4,11] Jevgenijs Lusciks,[3,5]
Joseph R. Broucek,[6] Josef W. Goldufsky,[3] Tasha Hughes,[6] Janet P. Zayas,[3] Hubert Dolubizno,[3] Ryan T. Sowell,[3]
Regina Kühner,[3] Sarah Burd,[7] John C. Kubasiak,[6] Arman Nabatiyan,[3,5] Sh'Rae Marshall,[1] Praveen K. Bommareddy,[1]
Shengguo Li,[1] Jenna H. Newman,[1] Claude E. Monken,[1,2] Sasha H. Shafikhani,[3] Amanda L. Marzo,[3,5]
Jose A. Guevara-Patino,[8] Ahmed Lasfar,[1,9] Paul G. Thomas,[10] Edmund C. Lattime,[1,2] Howard L. Kaufman,[1,2]
and Andrew Zloza[1,2,12,*]

[1]Section of Surgical Oncology, Division of Surgical Oncology Research, Rutgers Cancer Institute of New Jersey, New Brunswick,
NJ 08903, USA
[2]Department of Surgery, Rutgers Robert Wood Johnson Medical School, New Brunswick, NJ 08903, USA
[3]Department of Immunology/Microbiology, Rush University Medical Center, Chicago, IL 60612, USA
[4]Department of Microbiology and Immunology, University of Minnesota, Minneapolis, MN 55455, USA
[5]Department of Internal Medicine, Rush University Medical Center, Chicago, IL 60612, USA
[6]Department of General Surgery, Rush University Medical Center, Chicago, IL 60612, USA
[7]University of Oxford, Oxford OX1 2JD, UK
[8]Department of Surgery, Immunology Institute, Cardinal Bernardin Cancer Center, Loyola University Chicago, Maywood, IL 60153, USA
[9]Department of Pharmacology and Toxicology, Ernest Mario School of Pharmacy, Rutgers, The State University of New Jersey, Piscataway,
NJ 08854, USA
[10]Department of Immunology, St. Jude Children's Research Hospital, Memphis, TN 38105, USA
[11]Co-first author
[12]Lead Contact
*Correspondence: andrew.zloza@rutgers.edu
http://dx.doi.org/10.1016/j.celrep.2016.09.068

SUMMARY

In light of increased cancer prevalence and cancer-specific deaths in patients with infections, we investigated whether infections alter anti-tumor immune responses. We report that acute influenza infection of the lung promotes distal melanoma growth in the dermis and leads to accelerated cancer-specific host death. Furthermore, we show that during influenza infection, anti-melanoma CD8^{+} T cells are shunted from the tumor to the infection site, where they express high levels of the inhibitory receptor programmed cell death protein 1 (PD-1). Immunotherapy to block PD-1 reverses this loss of anti-tumor CD8^{+} T cells from the tumor and decreases infection-induced tumor growth. Our findings show that acute non-oncogenic infection can promote cancer growth, raising concerns regarding acute viral illness sequelae. They also suggest an unexpected role for PD-1 blockade in cancer immunotherapy and provide insight into the immune response when faced with concomitant challenges.

INTRODUCTION

Our current understanding of immunity relies principally on studies in which a single type of challenge or re-challenge is made to the immune system. Such work has been instrumental in deconstructing complicated immune cell functions and intricate molecular signaling networks. However, the immune system is often tasked with responding to multiple concomitant challenges, and how one type of challenge dictates the immune response to another is not well understood.

The majority of the work thus far on concomitant challenges has been done in the context of pathogenic co-infections, and findings in this field are discordant (Kenney et al., 2015; Mueller et al., 2007; Osborne et al., 2014; Stelekati et al., 2014). Further, although infections and cancers are two of the most common human maladies and cancer patients are at increased risk of infections, very little information is available regarding the consequences of concomitant non-oncogenic infection and cancer; thus, this subject is a matter of ongoing debate (Cooksley et al., 2005; Kohler et al., 1990; Wong et al., 2010). Case studies performed in the late 19th century report cancer regression in the context of infection-like reactions (e.g., in response to Coley's toxin), and recent work proposes that anti-tumor T cell populations can be expanded as a by-product of infection (Coley, 1891; Garrett, 2015; Iheagwara et al., 2014). However, emerging epidemiological studies report an increased prevalence of cancers and increased cancer-specific death in patients with infection (Attiê et al., 2014; Cox et al., 2010; Crum-Cianflone et al., 2009; Huang et al., 2013; Su et al., 2011; Swaminathan et al., 2015).

Therefore, toward advancing the scientific understanding of immunity in the context of multiple concomitant challenges, we investigated the effect of acute, non-oncogenic,

non-immune-destructive infection in one tissue on anti-cancer immune responses in a distal tissue. Surprisingly, we uncovered a potentially common mechanism of immune disruption in cancer-bearing hosts, namely the shunting of anti-tumor CD8+ T cells from the tumor microenvironment to the site of infection by acute non-oncogenic pathogens, an unexpected mechanism of programmed cell death protein 1 (PD-1) blockade in the treatment of cancer, and an important perspective to our basic understanding of the immune response in the context of concomitant challenges.

RESULTS AND DISCUSSION

Acute Influenza Infection Leads to Accelerated Cancer-Specific Host Death

To determine the impact of viral infection on cancer-specific mortality, we inoculated B6 mice with influenza 3 days before distal tumor challenge with B16 melanoma (Figure 1A). Influenza infection significantly accelerated cancer-specific host death ($p < 0.001$; Figure 1A). Furthermore, influenza infection as many as 30 days before tumor challenge likewise accelerated host death, albeit to a smaller degree compared with infection 3 days before tumor challenge (Figure 1B). Cancer-specific mortality was similar in mice infected and not infected with influenza 60 days before tumor challenge (Figure 1C). These data demonstrate that acute influenza infection leads to accelerated cancer-specific host death.

Influenza Infection Accelerates the Death of Hosts with Established Tumors and Leads to the Emergence of Otherwise Controlled Tumors

To determine whether influenza similarly affects established tumor growth, we challenged mice with B16 melanoma and then infected them 3 or 7 days later with influenza. Here, influenza infection of hosts with established tumors likewise accelerated cancer-specific host death (Figure 1D).

To determine whether infection could lead to the emergence of cancer that is otherwise controlled by the immune system, we challenged mice with suboptimal cell numbers of B16 (12,000 and 1,200) at which the percentage of tumor-free mice is increased (to 60% and 100%, respectively) compared with our optimal challenge with 120,000 cells (Figure 1E). Here, influenza infection significantly decreased the percentage of tumor-free mice at both 12,000 and 1,200 B16 cell challenges to 0% ($p < 0.05$ and $p < 0.01$, respectively; Figure 1E). These data show that concomitant influenza accelerates the death of hosts with established tumors and leads to the emergence of otherwise controlled tumors.

Infection-Accelerated Tumor Growth and Host Death Occur in the Context of Various Pathogens and Cancers

To determine whether these findings are more broadly applicable, we challenged mice with a series of pathogens, administered through different sites of infection and via varying routes of delivery. Acute lymphocytic choriomeningitis virus (LCMV; Armstrong strain) infection, which infects the spleen, liver, and kidneys and is administered via intraperitoneal (i.p.) injection (Ahmed et al., 1984), results in significantly accelerated host

death ($p < 0.001$; Figure 2A). Furthermore, this phenomenon is not restricted to viruses because concomitant bacterial infection with *Staphylococcus aureus* also hastened tumor growth ($p < 0.05$; Figure 2B). These findings are not restricted to transplantable tumor models, because in a genetically driven mouse model of melanoma (utilizing heterozygous Braf/PTEN mice), increased melanoma was observed in mice infected with influenza and complete penetrance was observed when tamoxifen and influenza were combined (Figure 2C). To assess whether the results observed are applicable to a cancer of another type, in a different tissue, and in a different mouse strain, we determined the effects of influenza infection on 4T1 breast cancer in the mammary fat pad of Balb/c mice. Here, influenza infection significantly increased tumor growth ($p < 0.05$) (Figure 2D). Collectively, these data show that infection-accelerated tumor growth and host death occur in the following various contexts: (1) tumor types, (2) sites of tumor challenge, (3) mouse strains, (4) infectious agents, (5) sites of infection, and (6) models of tumor induction.

Anti-tumor CD8+ T Cells Are Shunted to the Lung during Influenza Infection

CD8+ T cells are important mediators of immunity, tasked with clearing both viral infections and tumors. Therefore, to elucidate the mechanism by which influenza infection promotes tumor growth and reduces survival, we determined the proportion of anti-tumor CD8+ T cells within the tumor and at the infection site. To track anti-tumor CD8+ T cells, we adoptively transferred Thy1.1+ Pmel CD8+ T cells specific against melanoma gp100$_{25-33}$ into Thy1.1− B6 mice (Figure 3A). Surprisingly, in mice infected with influenza, Pmel CD8+ T cells were significantly reduced on day 15 in the tumor compared with uninfected hosts ($p < 0.01$) and found at high levels at the site of infection ($p < 0.001$; Figures 3B and 3C). Similar findings were observed in terms of Pmel CD8+ T cell numbers in the tumor and lungs (Figure 3D), but were not observed in tissues unrelated to the tumor challenge or infection (Figure 3E).

To determine whether anti-tumor CD8+ T cells could traffic from the tumor to the influenza-infected lungs, we transplanted tumors from uninfected B16 melanoma-bearing B6 mice (that previously received an adoptive transfer of Pmel CD8+ T cells) to naive B6 mice that were subsequently influenza-infected or left uninfected (Figure 3F). Influenza infection resulted in the significant accumulation of tumor-specific (Pmel) CD8+ T cells from the transplanted tumors in the influenza-infected lungs ($p < 0.01$) but not spleen (Figure 3G). This finding shows that anti-tumor CD8+ T cells are shunted by a distal infection from the tumor to the site of infection.

Disruption of Anti-tumor Responses Is Not Due to Tumor-Induced Immune Suppression of Viral Clearance or the Inability of the Immune System to Respond to Concomitant Challenges

To assess whether the observed disruption of anti-tumor responses leading to accelerated cancer-specific death is due to tumor-induced immune suppression, we inoculated two groups of B6 mice with influenza and challenged one of those groups with distal B16 melanoma. Notably, tumor challenge did not suppress the immune clearance of influenza (Figure S1A),
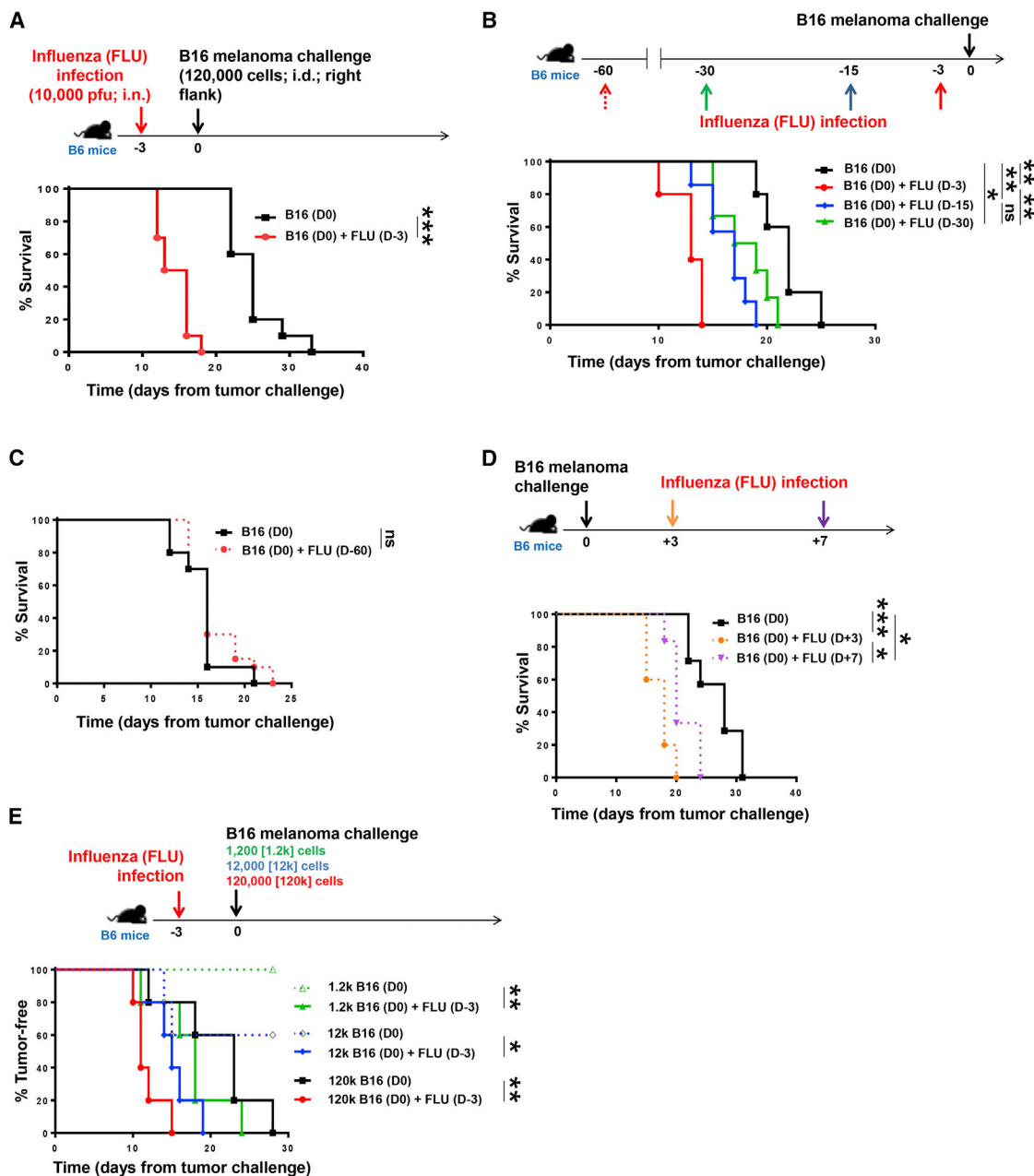
Figure 1. Influenza Infection Results in Accelerated Melanoma-Specific Host Death

(A) Experimental design (top). Survival of B6 mice infected on day −3 with influenza and challenged with B16 melanoma on day 0 via intradermal (i.d.) injection (bottom).
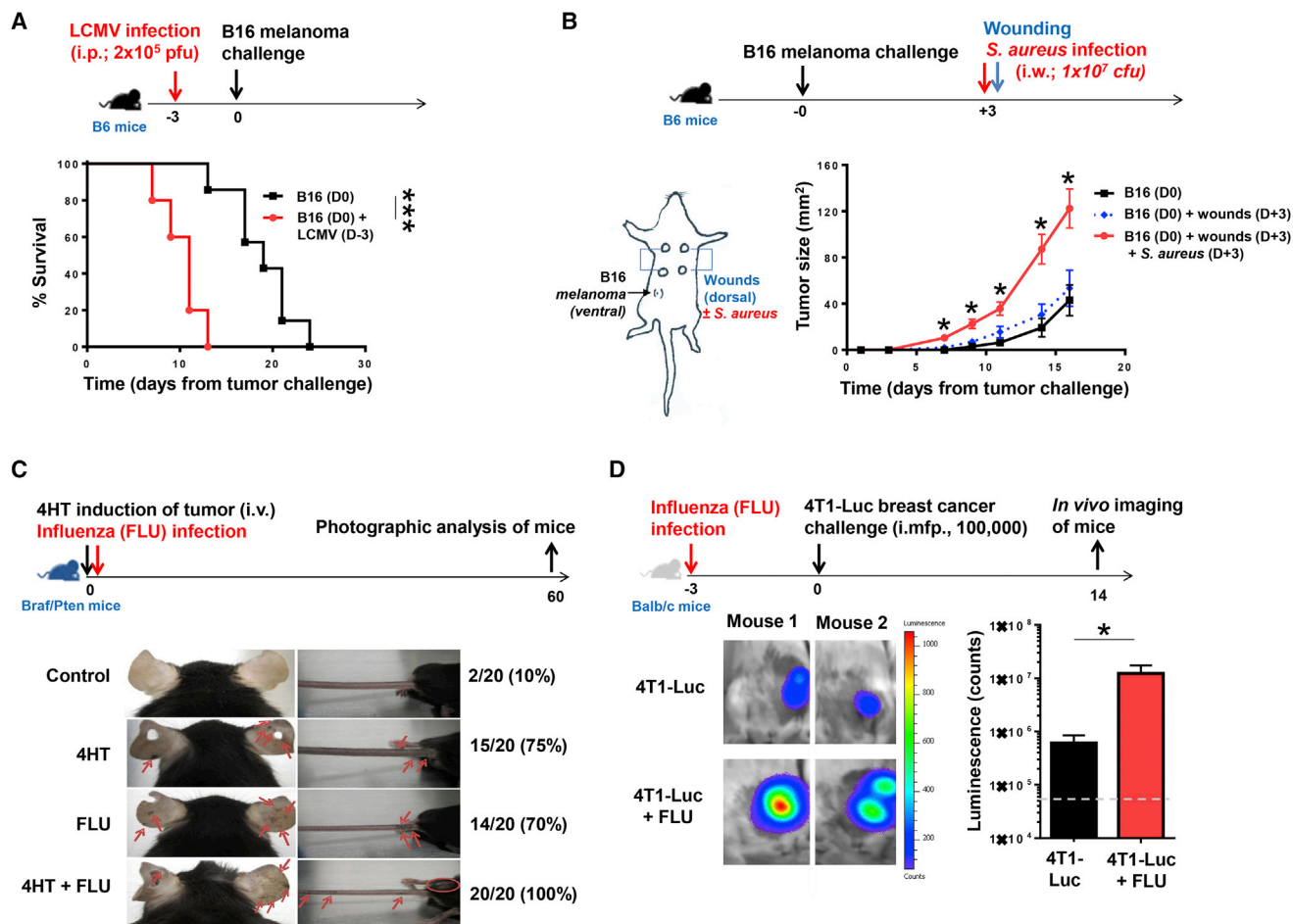
(B) Experimental design (top). Survival of B6 mice infected on days −3, −15, or −30 with influenza and challenged with B16 melanoma on day 0 (bottom).

(C) Survival of B6 mice infected on day −60 with influenza and challenged with B16 melanoma on day 0.

(D) Experimental design (top). Survival of B6 mice infected on days +3 or +7 with influenza and challenged with B16 melanoma on day 0 (bottom).

(E) Experimental design (top). Percentage of B6 mice remaining tumor-free after infection on day −3 with influenza and challenge with B16 melanoma (120,000, 12,000, or 1,200 cells) on day 0 (bottom).

All experiments were performed with 7–10 mice per group with at least two independent repeat experiments. Survival was defined by tumor size < 100 mm^2. *p < 0.05; **p < 0.01; ***p < 0.001. ns, not significant.

Figure 2. Pathogenic Infections Accelerate Tumor Growth in the Context of Various Cancers

(A) Experimental design (top). Survival of B6 mice infected with LCMV (Armstrong strain) on day −3 and challenged with B16 melanoma on day 0 via intradermal (i.d.) injection (bottom). Survival was defined by tumor size < 100 mm^2.

(B) Experimental design (top) and wound and infection diagram (bottom left). Tumor growth in B6 mice challenged with B16 melanoma on day 0, wounded on day +3, and infected at day +3 with *Staphylococcus aureus* via intra-wound (i.w.) injection (bottom right).

(C) Experimental design (top). Tumor incidence in Braf/PTEN mice infected at 8 weeks of age with influenza and/or treated with 4HT on day 0. Representative images and number and percentages of mice with one or more observed tumors on day 60 from two combined experiments (bottom). Red arrows and circle indicate areas of melanoma growth.

(D) Experimental design (top). Balb/c mice were infected on day −3 with influenza and challenged with 4T1-Luciferase (4T1-Luc) murine breast cancer cells on day 0 via intra-mammary fat pad (i.mfp.) injection. Tumor growth was measured using the live imaging IVIS system (bottom). Results are depicted with representative luminescence images (bottom left) and cumulative bar graphs (bottom right). Dashed line depicts background luminescence.

All experiments were performed with 5–10 mice per group with at least two independent repeat experiments. *p < 0.05; ***p < 0.001. Error bars represent the SEM.

demonstrating that cancer in these hosts does not significantly suppress the anti-viral response.

To determine whether accelerated cancer-specific death is due to a general inability of the immune system to respond to concomitant challenges, we infected B6 mice on day −3 with influenza and/or with vaccinia virus (VACV) on day 0. Importantly, influenza infection did not alter the natural clearance of VACV (Figure S1B) or the proportion of VACV-tetramer+ CD8+ T cells at the site of influenza infection (Figures S1C and S1D), suggesting that influenza infection does not in general prevent concomitant disease clearance, but does accelerate tumor growth in our studies.

Therapeutic Blockade of PD-1 Results in Reversal of Infection-Mediated Anti-tumor Response Disruption

Based on the extended period of time necessary after infection clearance for anti-tumor immune responses to be recovered (Figures 1B and 1C), we hypothesized that infection leads to the dysfunction of anti-tumor CD8+ T cells shunted to the site of infection. Because exhaustion is a hallmark of dysfunctional anti-tumor CD8+ T cells (Ahmadzadeh et al., 2009; Sakuishi et al., 2010; Wherry et al., 2007), we determined the expression of activation and exhaustion receptor, PD-1, on tumor-specific CD8+ T cells. Although PD-1 expression was observed on anti-tumor Pmel CD8+ T cells in the tumor (10%–20%; A.Z.,
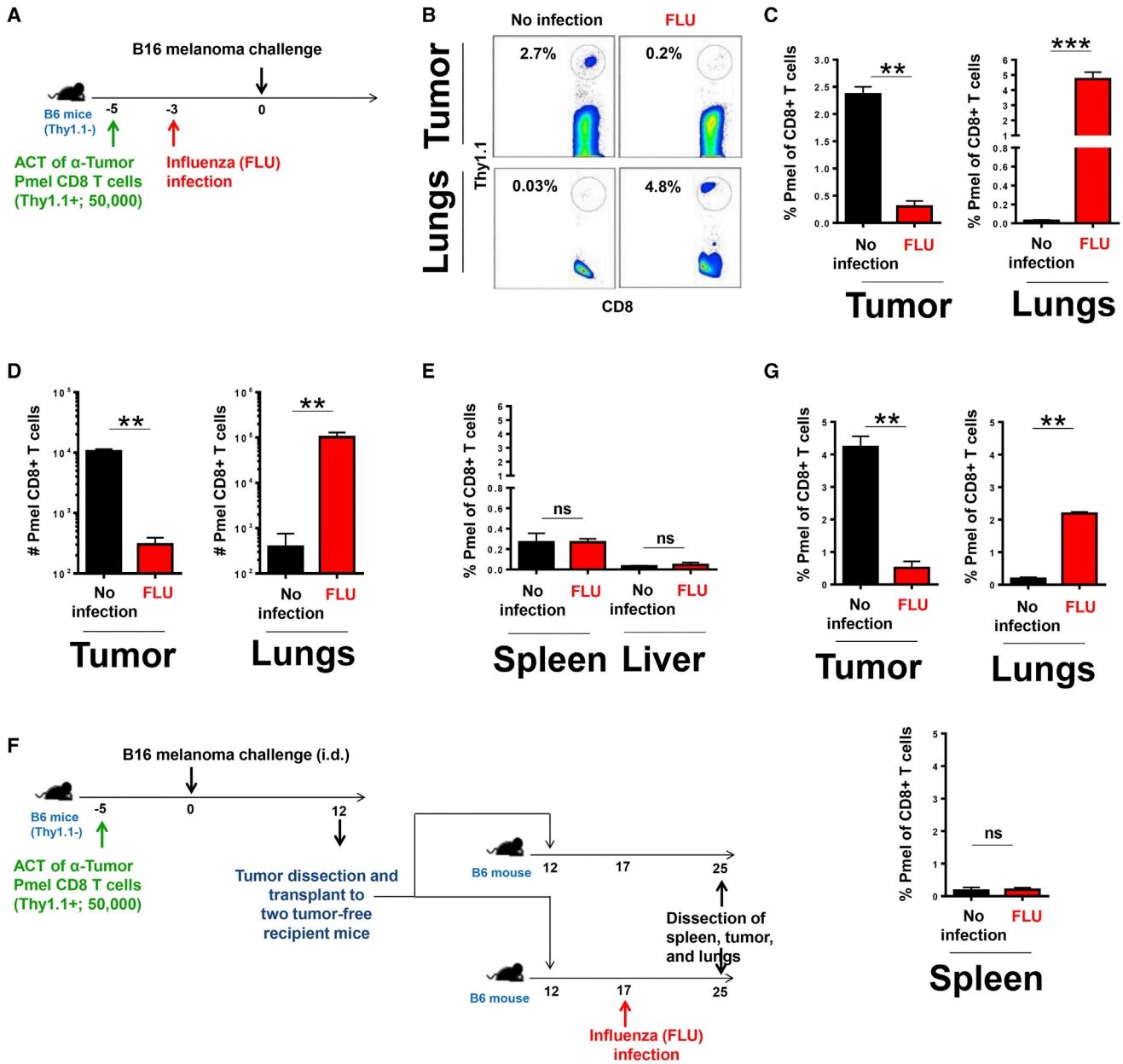
Figure 3. Melanoma-Specific CD8^{+} T Cells Are Shunted from the Tumor to the Site of Infection

(A) Experimental design for studies in which B6 mice received adoptive cell transfer (ACT) of Pmel cells on day −5, were infected with influenza on day −3, and were challenged with B16 melanoma on day 0.

(B) Tumors from experiment described in (A) were resected at day 15 and analyzed via flow cytometry. Results depicted by representative flow plots show % of Pmel CD8^{+} T cells among all CD8^{+} T cells. Axes on all plots are log scale.

(C) Cumulative bar graphs showing percentage of Pmel CD8^{+} T cells determined from the experiment described in (A).

(D) Cumulative bar graphs showing number of Pmel CD8^{+} T cells determined from the experiment described in (A).

(E) Cumulative bar graphs showing percentage of Pmel CD8^{+} T cells determined from the experiment described in (A).

(F) Experimental design for studies in which B6 mice (Thy1.1−; donor mice) received ACT of Pmel cells (Thy1.1+) on day −5 and were challenged with B16 melanoma on day 0. On day 12, each tumor (∼36 mm[2]) was resected and transplanted into the intradermal space of the right flank of two naive B6 mice (recipient mice). On day 17, one of two naive B6 tumor-recipient mice from each pair was infected with influenza.

(G) Tumor, lungs, and spleen from mice in the experiment described in (F) were resected on day 25, and the presence of Pmel CD8^{+} T cells was determined by flow cytometry.

All experiments were performed with 5–10 mice per group with at least two independent repeat experiments. **p < 0.01; ***p < 0.001. ns, not significant. Error bars represent the SEM.

unpublished data), a greater proportion of anti-tumor CD8^{+} T cells expressed PD-1 in the infected lung even when compared with influenza-ovalbumin (OVA) infection-specific (OT-I) CD8^{+} T cells in the lungs (p < 0.01) (Figures 4A–4C). Based on this finding and the use of PD-1 blockade in the clinical treatment of melanoma (Hamid et al., 2013), lung cancer (Rizvi et al., 2015), and prostate cancer (Topalian et al., 2012), we investigated whether such systemic blockade in the context of influenza infection would lead to recovered anti-tumor CD8^{+} T cell responses in the tumor. PD-1 blockade (on days 0 and 2; 100 μg/mouse/day) decelerated tumor growth in influenza-infected mice to the rate observed in untreated uninfected mice (Figure 4D). Further, PD-1 blockade rescued the percentage of anti-tumor CD8^{+} T cells within the tumor (Figures 4E and 4F). These data demonstrate that anti-tumor CD8^{+} T cells shunted to the site of infection upregulate activation and exhaustion marker, PD-1, and that its therapeutic blockade results in reversal of the acceleration of tumor growth by infection.

Conclusions

Overall, our findings demonstrate that acute, non-oncogenic infection of an unrelated tissue (i.e., distal to the tumor site) results in accelerated tumor growth and hastened host death from cancer. Based on our observations, a mechanism by which infection impedes anti-tumor responses includes the shunting of anti-tumor CD8^{+} T cell responses from the tumor to the site of infection. The exact means by which this occurs may involve non-specific CD8^{+} T cell trafficking to another (or greater) site of inflammation (e.g., via a chemokine gradient), where tumor-specific CD8^{+} T cells become hyper-activated or exhausted (as illustrated by increased PD-1 expression at the site of infection) and are unable to aid in the immune response at the tumor site. Recent studies demonstrating antigen epitopes shared between some infections and cancers (Snyder et al., 2014) may also explain the observed shunting of CD8^{+} T cells from the tumor to the infection site. Further, mechanisms yet to be determined may be involved in driving the decision-making process of the immune system in the context of concomitant challenges.

Our findings define a previously unrecognized and potentially common mechanism of immune disruption in cancer-bearing hosts, namely acute non-oncogenic viral infection. This finding is important because it raises concerns regarding previously unrecognized sequelae of acute viral illness, it highlights an unexpected mechanism of PD-1 blockade in the treatment of cancer, it may explain epidemiological findings describing increased cancer prevalence and cancer-specific deaths in the context of infection, and it contributes to our basic understanding of the immune response in the context of concomitant challenges.

EXPERIMENTAL PROCEDURES

Mice and Adoptive Cell Transfers

C57BL/6 (B6; no. 00664), Balb/c (no. 00651), Braf/PTEN (no. 13590), Pmel (no. 5023), and OT-1 (no. 03831) mice, aged 6 to 8 weeks, from Jackson Laboratory, were housed in a specific pathogen-free facility at Rutgers Cancer Institute of New Jersey and/or Rush University Medical Center. Experiments involving animals were carried out in accordance with respective Institutional Animal Care and Use Committee and Institutional Biosafety Committee guide-

lines. Pmel (50,000) and OT-1 (50,000) cells were derived from the spleen and adoptively transferred via injection in 100 μl PBS into the retroorbital venous sinus.

Tumor Challenges and Monitoring

Mice (5–10 per group per experiment, as described for each experiment) were anesthetized with isoflurane and challenged with B16-F10 (1,200–120,000 cells, as described for each experiment) via intradermal (i.d.) injection in the right flank or 4T1-Luciferase (100,000 cells) via injection in the mammary fat pad, as previously described (Bellavance et al., 2011; Kohlhapp et al., 2012; Zloza et al., 2012). Before injection, these cells were cultured in RPMI 1640 plus 10% heat-inactivated fetal bovine serum (Atlanta Biologicals), 2 mM L-glutamine (Mediatech), and 1% penicillin/streptomycin (Mediatech). Tumor area (length × width) was measured using calipers. Survival of tumor-bearing mice was defined by tumor size < 100 mm², unless otherwise noted. For 4T1-luciferase experiments, mice were injected with 150 μg D-Luciferin (Sigma-Aldrich) in PBS, anesthetized with isoflurane, and imaged live with the IVIS system (Xenogen), as per manufacturer's instructions. For experiments involving Braf/PTEN mice, tumors were induced in some mice using 4-hydroxy tamoxifen (4HT; 1 mg) via intravenous (i.v.) injection (Dankort et al., 2009). For these experiments, all mice were 8 weeks old and were considered to be melanoma-positive if one or more dermal melanomas were observed at day 60. In some experiments, tumors, spleens, and/or lungs were obtained.

Tumor Transplantation Experiments

For tumor transplantation experiments, naive B6 mice (hereafter termed "donor mice"; Thy1.1^{−}) received an adoptive transfer of Pmel CD8^{+} T cells (into the retroorbital venous sinus; 50,000 cells; Thy1.1^{+}) on day −5 and were challenged on day 0 with B16 melanoma (i.d. injection; 120,000 cells). On day 12, B16 tumors (with infiltrating Thy1.1^{+} Pmel CD8^{+} T cells) were dissected from donor B6 mice and transplanted into the flank i.d. space (equal size) of a pair (i.e., two) of tumor-free B6 mice ("recipient mice"; Thy1.1[−]). On day 17, one mouse of each recipient pair was left uninfected (control; PBS administration), and the other mouse of each recipient pair received influenza infection (10,000 plaque-forming unit [PFUs] via intranasal administration). On day 25, all recipient mice were euthanized and lungs were dissected.
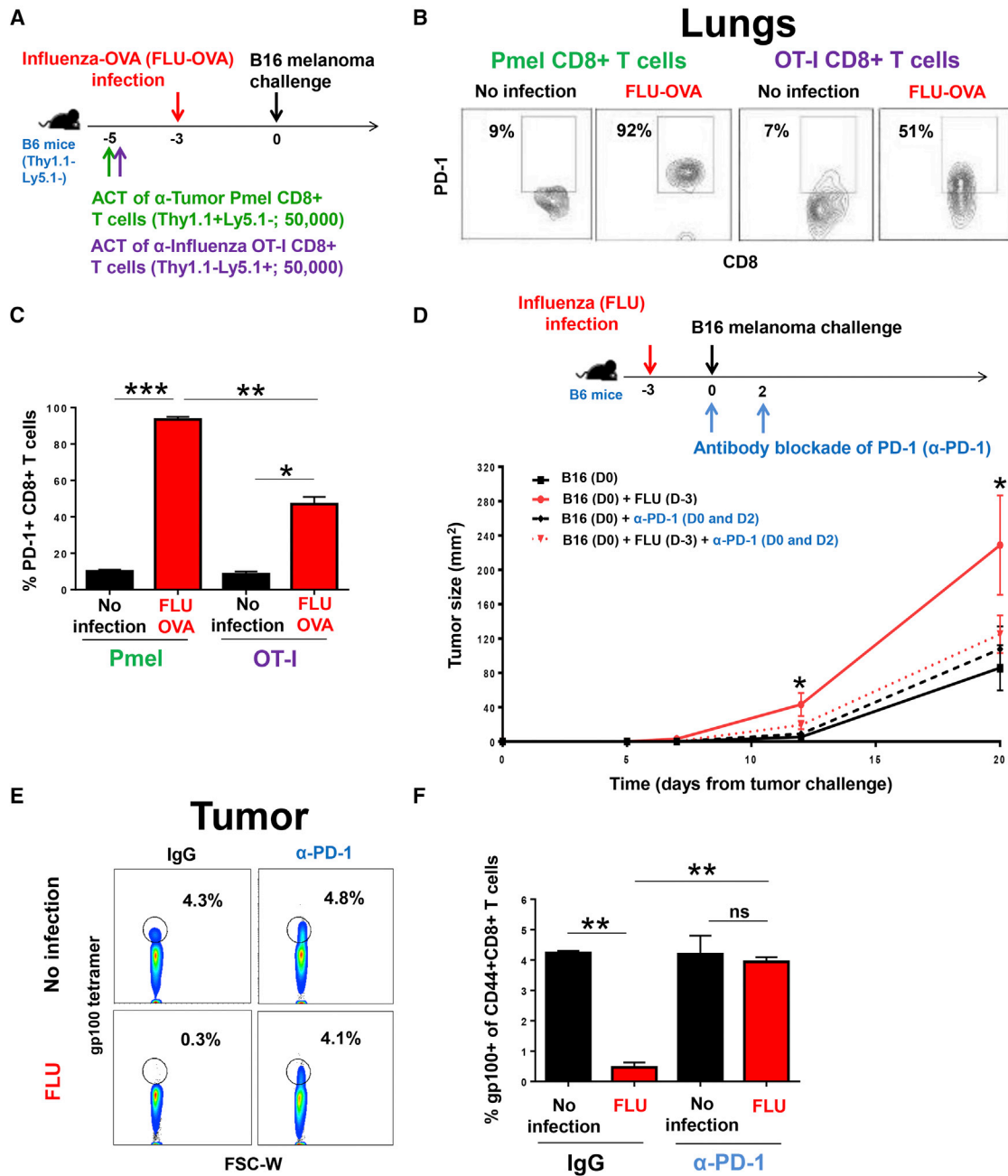
Infections and PD-1 Blockade

For influenza infections, mice were inoculated (10,000 PFUs in 40 μl) with influenza A/H1N1/PR8 or influenza-OVA (A/H1N1/PR8-OVA) via intranasal administration (Rutigliano et al., 2014). For LCMV infections, mice were inoculated with LCMV Armstrong strain (2 × 10⁵ PFUs) by i.p. injection. For *Staphylococcus aureus* (strain COL) skin infections, a 5-mm biopsy punch was used to create four full-thickness wounds in the dorsal skin of mice, opposite from the ventral site of the tumor (Kroin et al., 2015). *Staphylococcus aureus* was applied to the wounds (1 × 10⁷ colony-forming units [CFUs] in 10 μl PBS). Mice were housed in individual cages after wounding to prevent cross-contamination. For VACV skin infections, B6 mice were inoculated with VACV (NYCBH strain) via i.d. injection (10⁶ PFUs) and analyzed by plaque assays (Zhang et al., 2006). For PD-1 blockade, anti-PD-1 (250 μg; clone RMP1-14; BioXCell) or matched IgG control antibody was administered via i.p. injection.

Flow Cytometry and Staining

Cell staining data were collected with the Canto II flow cytometer (BD) and analyzed with FlowJo software (Tree Star) as previously described (Zloza et al., 2012), and tissue-parenchyma (i.e., non-vascular) cells were identified by in vivo antibody labeling of cells within the vasculature (Anderson et al., 2014). All antibodies were purchased from eBioscience.

Statistical Analysis

Kaplan-Meier curves were used to present animal survival and tumor incidence data, and log rank test was used to compare such curves. Unless otherwise noted, Student's t test (two-tailed) was used. All analyses were performed using Prism software (v4.0, GraphPad). A p value < 0.05 was considered to denote statistically significant differences.

Figure 4. PD-1 Blockade Rescues Anti-tumor Responses Impeded by Infection

(A) Experimental design for studies in which B6 mice (Thy1.1⁻Ly5.1⁻) received an adoptive cell transfer (ACT) on day −5 of Pmel cells (Thy1.1$^+$Ly5.1$^-$) and OT-I cells (Thy1.1⁻Ly5.1$^+$) via intravenous (i.v.) injection, were infected on day −3 with influenza-OVA, and challenged with B16 melanoma on day 0.

(B) Lungs from experiment described in (A) were resected at day 10, and PD-1 expression by Pmel and OT-I CD8$^+$ T cells was determined by flow cytometry as shown in representative flow plots. Axes on all plots are log scale.

(C) Cumulative bar graphs showing percentage of Pmel CD8$^+$ T cells determined from the experiment described in (A).

(D) Experimental design (top). B6 mice were infected with influenza (FLU) at day −3 and challenged with B16 melanoma via intradermal (i.d.) injection. No adoptive transfer of CD8$^+$ T cells was conducted in this experiment. Some mice were treated with PD-1 blocking antibody (anti-PD-1, 100 μg) on days 0 and 2 (bottom).

(E) Tumors were resected at day 20, and endogenous melanoma-specific CD8$^+$ T cells were identified using gp100$_{25-33}$ tetramer staining after gating on CD8$^+$CD44$^+$ T cells, as shown in the representative flow plots. y axis on all plots is log scale; x axis is linear scale.

(F) Cumulative bar graphs showing % of Pmel CD8$^+$CD44$^+$ T cells determined from the experiment described in (E).

All experiments were performed with 5–10 mice per group with at least two independent repeat experiments. *p < 0.05; **p < 0.01; ***p < 0.001. ns, not significant. Error bars represent the SEM.

SUPPLEMENTAL INFORMATION

Supplemental Information includes one figure and can be found with this article online at http://dx.doi.org/10.1016/j.celrep.2016.09.068.

REFERENCES

Ahmadzadeh, M., Johnson, L.A., Heemskerk, B., Wunderlich, J.R., Dudley, M.E., White, D.E., and Rosenberg, S.A. (2009). Tumor antigen-specific CD8 T cells infiltrating the tumor express high levels of PD-1 and are functionally impaired. Blood *114*, 1537–1544.

Ahmed, R., Salmi, A., Butler, L.D., Chiller, J.M., and Oldstone, M.B. (1984). Selection of genetic variants of lymphocytic choriomeningitis virus in spleens of persistently infected mice. Role in suppression of cytotoxic T lymphocyte response and viral persistence. J. Exp. Med. *160*, 521–540.

Anderson, K.G., Mayer-Barber, K., Sung, H., Beura, L., James, B.R., Taylor, J.J., Qunaj, L., Griffith, T.S., Vezys, V., Barber, D.L., and Masopust, D. (2014). Intravascular staining for discrimination of vascular and tissue leukocytes. Nat. Protoc. *9*, 209–222.

Attiè, R., Chinen, L.T., Yoshioka, E.M., Silva, M.C., and de Lima, V.C. (2014). Acute bacterial infection negatively impacts cancer specific survival of colorectal cancer patients. World J. Gastroenterol. *20*, 13930–13935.

Bellavance, E.C., Kohlhapp, F.J., Zloza, A., O'Sullivan, J.A., McCracken, J., Jagoda, M.C., Lacek, A.T., Posner, M.C., and Guevara-Patino, J.A. (2011). Development of tumor-infiltrating CD8+ T cell memory precursor effector cells and antimelanoma memory responses are the result of vaccination and TGF-β blockade during the perioperative period of tumor resection. J. Immunol. *186*, 3309–3316.

Coley, W.B. (1891). II. Contribution to the knowledge of sarcoma. Ann. Surg. *14*, 199–220.

Cooksley, C.D., Avritscher, E.B., Bekele, B.N., Rolston, K.V., Geraci, J.M., and Elting, L.S. (2005). Epidemiology and outcomes of serious influenza-related infections in the cancer population. Cancer *104*, 618–628.

Cox, B., Richardson, A., Graham, P., Gislefoss, R.E., Jellum, E., and Rollag, H. (2010). Breast cancer, cytomegalovirus and Epstein-Barr virus: a nested case-control study. Br. J. Cancer *102*, 1665–1669.

Crum-Cianflone, N., Hullsiek, K.H., Marconi, V., Weintrob, A., Ganesan, A., Barthel, R.V., Fraser, S., Agan, B.K., and Wegner, S. (2009). Trends in the incidence of cancers among HIV-infected persons and the impact of antiretroviral therapy: a 20-year cohort study. AIDS *23*, 41–50.

Dankort, D., Curley, D.P., Cartlidge, R.A., Nelson, B., Karnezis, A.N., Damsky, W.E., Jr., You, M.J., DePinho, R.A., McMahon, M., and Bosenberg, M. (2009). Braf(V600E) cooperates with Pten loss to induce metastatic melanoma. Nat. Genet. *41*, 544–552.

Garrett, W.S. (2015). Cancer and the microbiota. Science *348*, 80–86.

Hamid, O., Robert, C., Daud, A., Hodi, F.S., Hwu, W.J., Kefford, R., Wolchok, J.D., Hersey, P., Joseph, R.W., Weber, J.S., et al. (2013). Safety and tumor responses with lambrolizumab (anti-PD-1) in melanoma. N. Engl. J. Med. *369*, 134–144.

Huang, J., Magnusson, M., Törner, A., Ye, W., and Duberg, A.S. (2013). Risk of pancreatic cancer among individuals with hepatitis C or hepatitis B virus infection: a nationwide study in Sweden. Br. J. Cancer *109*, 2917–2923.

Iheagwara, U.K., Beatty, P.L., Van, P.T., Ross, T.M., Minden, J.S., and Finn, O.J. (2014). Influenza virus infection elicits protective antibodies and T cells specific for host cell antigens also expressed as tumor-associated antigens: a new view of cancer immunosurveillance. Cancer Immunol. Res. *2*, 263–273.

Kenney, L.L., Cornberg, M., Chen, A.T., Emonet, S., de la Torre, J.C., and Selin, L.K. (2015). Increased immune response variability during simultaneous viral coinfection leads to unpredictability in CD8 T cell immunity and pathogenesis. J. Virol. *89*, 10786–10801.

Kohler, M., Rüttner, B., Cooper, S., Hengartner, H., and Zinkernagel, R.M. (1990). Enhanced tumor susceptibility of immunocompetent mice infected with lymphocytic choriomeningitis virus. Cancer Immunol. Immunother. *32*, 117–124.

Kohlhapp, F.J., Zloza, A., O'Sullivan, J.A., Moore, T.V., Lacek, A.T., Jagoda, M.C., McCracken, J., Cole, D.J., and Guevara-Patiño, J.A. (2012). CD8(+) T cells sabotage their own memory potential through IFN-γ-dependent modification of the IL-12/IL-15 receptor α axis on dendritic cells. J. Immunol. *188*, 3639–3647.

Kroin, J.S., Buvanendran, A., Li, J., Moric, M., Im, H.J., Tuman, K.J., and Shafikhani, S.H. (2015). Short-term glycemic control is effective in reducing surgical site infection in diabetic rats. Anesth. Analg. *120*, 1289–1296.

Mueller, S.N., Hosiawa-Meagher, K.A., Konieczny, B.T., Sullivan, B.M., Bachmann, M.F., Locksley, R.M., Ahmed, R., and Matloubian, M. (2007). Regulation of homeostatic chemokine expression and cell trafficking during immune responses. Science *317*, 670–674.

Osborne, L.C., Monticelli, L.A., Nice, T.J., Sutherland, T.E., Siracusa, M.C., Hepworth, M.R., Tomov, V.T., Kobuley, D., Tran, S.V., Bittinger, K., et al. (2014). Coinfection. Virus-helminth coinfection reveals a microbiota-independent mechanism of immunomodulation. Science *345*, 578–582.

Rizvi, N.A., Mazières, J., Planchard, D., Stinchcombe, T.E., Dy, G.K., Antonia, S.J., Horn, L., Lena, H., Minenza, E., Mennecier, B., et al. (2015). Activity and safety of nivolumab, an anti-PD-1 immune checkpoint inhibitor, for patients with advanced, refractory squamous non-small-cell lung cancer (CheckMate 063): a phase 2, single-arm trial. Lancet Oncol. *16*, 257–265.

Rutigliano, J.A., Sharma, S., Morris, M.Y., Oguin, T.H., 3rd, McClaren, J.L., Doherty, P.C., and Thomas, P.G. (2014). Highly pathological influenza A virus infection is associated with augmented expression of PD-1 by functionally compromised virus-specific CD8+ T cells. J. Virol. *88*, 1636–1651.

Sakuishi, K., Apetoh, L., Sullivan, J.M., Blazar, B.R., Kuchroo, V.K., and Anderson, A.C. (2010). Targeting Tim-3 and PD-1 pathways to reverse T cell exhaustion and restore anti-tumor immunity. J. Exp. Med. *207*, 2187–2194.

Snyder, A., Makarov, V., Merghoub, T., Yuan, J., Zaretsky, J.M., Desrichard, A., Walsh, L.A., Postow, M.A., Wong, P., Ho, T.S., et al. (2014). Genetic basis for clinical response to CTLA-4 blockade in melanoma. N. Engl. J. Med. *371*, 2189–2199.

Stelekati, E., Shin, H., Doering, T.A., Dolfi, D.V., Ziegler, C.G., Beiting, D.P., Dawson, L., Liboon, J., Wolski, D., Ali, M.A., et al. (2014). Bystander chronic infection negatively impacts development of CD8(+) T cell memory. Immunity *40*, 801–813.

Su, F.H., Chang, S.N., Chen, P.C., Sung, F.C., Su, C.T., and Yeh, C.C. (2011). Association between chronic viral hepatitis infection and breast cancer risk: a nationwide population-based case-control study. BMC Cancer *11*, 495.

Swaminathan, S., Klemm, L., Park, E., Papaemmanuil, E., Ford, A., Kweon, S.M., Trageser, D., Hasselfeld, B., Henke, N., Mooster, J., et al. (2015). Mechanisms of clonal evolution in childhood acute lymphoblastic leukemia. Nat. Immunol. *16*, 766–774.

Topalian, S.L., Hodi, F.S., Brahmer, J.R., Gettinger, S.N., Smith, D.C., McDermott, D.F., Powderly, J.D., Carvajal, R.D., Sosman, J.A., Atkins, M.B., et al. (2012). Safety, activity, and immune correlates of anti-PD-1 antibody in cancer. N. Engl. J. Med. *366*, 2443–2454.

Wherry, E.J., Ha, S.J., Kaech, S.M., Haining, W.N., Sarkar, S., Kalia, V., Subramaniam, S., Blattman, J.N., Barber, D.L., and Ahmed, R. (2007). Molecular signature of CD8+ T cell exhaustion during chronic viral infection. Immunity *27*, 670–684.

Wong, A., Marrie, T.J., Garg, S., Kellner, J.D., and Tyrrell, G.J.; SPAT Group (2010). Increased risk of invasive pneumococcal disease in haematological and solid-organ malignancies. Epidemiol. Infect. *138*, 1804–1810.

Zhang, H., Monken, C.E., Zhang, Y., Lenard, J., Mizushima, N., Lattime, E.C., and Jin, S. (2006). Cellular autophagy machinery is not required for vaccinia virus replication and maturation. Autophagy *2*, 91–95.

Zloza, A., Kohlhapp, F.J., Lyons, G.E., Schenkel, J.M., Moore, T.V., Lacek, A.T., O'Sullivan, J.A., Varanasi, V., Williams, J.W., Jagoda, M.C., et al. (2012). NKG2D signaling on CD8^{+} T cells represses T-bet and rescues CD4-unhelped CD8^{+} T cell memory recall but not effector responses. Nat. Med. *18*, 422–428.